Since January 2020 Elsevier has created a COVID-19 resource centre with free information in English and Mandarin on the novel coronavirus COVID-19. The COVID-19 resource centre is hosted on Elsevier Connect, the company's public news and information website.

Virology 479-480 (2015) 75–84

Contents lists available at ScienceDirect

Virology

journal homepage: www.elsevier.com/locate/yviro

Review

Silencing the alarms: Innate immune antagonism by rotavirus NSP1 and VP3

Marco Morelli, Kristen M. Ogden, John T. Patton *

Rotavirus Molecular Biology Section, Laboratory of Infectious Diseases, National Institute of Allergy and Infectious Diseases, National Institutes of Health, Bethesda, MD 20892, USA

ARTICLE INFO

Article history:
Received 3 December 2014
Returned to author for revisions
23 December 2014
Accepted 5 January 2015
Available online 25 February 2015

Keywords:
Rotavirus
Innate immunity
Interferon signaling pathway
OAS/RNase L pathway
β-TrCP
NF-κB
Viral E3 ubiquitin ligase
Viral phosphodiesterase

ABSTRACT

The innate immune response involves a broad array of pathogen sensors that stimulate the production of interferons (IFNs) to induce an antiviral state. Rotavirus, a significant cause of childhood gastroenteritis and a member of the *Reoviridae* family of segmented, double-stranded RNA viruses, encodes at least two direct antagonists of host innate immunity: NSP1 and VP3. NSP1, a putative E3 ubiquitin ligase, mediates the degradation of cellular factors involved in both IFN induction and downstream signaling. VP3, the viral capping enzyme, utilizes a 2H-phosphodiesterase domain to prevent activation of the cellular oligoadenylate synthase (OAS)/RNase L pathway. Computational, molecular, and biochemical studies have provided key insights into the structural and mechanistic basis of innate immune antagonism by NSP1 and VP3 of group A rotaviruses (RVA). Future studies with non-RVA isolates will be essential to understand how other rotavirus species evade host innate immune responses.

Published by Elsevier Inc.

Contents

Introduction

The innate immune response is the first line of defense after a pathogen has breached physical barriers and entered a host (Takeuchi and Akira, 2010). Cellular pathogen sensors known as

* Correspondence to: Laboratory of Infectious Diseases, NIAID/NIH, 50 South Drive, Room 6308, Bethesda, MD 20892, USA.
E-mail address: jpattn76@vt.edu (J.T. Patton).

http://dx.doi.org/10.1016/j.virol.2015.01.006
0042-6822/Published by Elsevier Inc.

pattern recognition receptors (PRRs)—these include Toll-like (TLRs), retinoic acid-inducible gene 1 (RIG-I)-like (RLRs), and nucleotide-binding organization domain (NOD)-like (NLRs) receptors—detect conserved microbial antigens, or pathogen-associated molecular patterns (PAMPs), to activate transcription factors that upregulate expression of proinflammatory cytokines such as interferons (IFNs). In response to viral infection, all cells can produce type I (IFN-α/β) and III (IFN-λ) IFNs, which signal in an autocrine and paracrine manner through the Janus kinase (JAK)-signal transducer and activator of transcription (STAT) pathway to upregulate expression of hundreds of IFN-stimulated genes (ISGs) and induce an antiviral state (Goubau et al., 2013; Taylor and Mossman, 2013). ISGs can restrict pathogenesis at all stages of the viral life cycle: entry and uncoating, transcription and translation, and assembly and egress (Goubau et al., 2013). Viruses have evolved a wealth of strategies to evade detection by PRRs and to directly antagonize the host innate immune response, which contribute to their continued success.

Rotavirus biology

Rotavirus (RV), a double-stranded RNA (dsRNA) virus of the *Reoviridae* family, is a significant cause of childhood gastroenteritis and accounts for ~450,000 deaths annually (Tate et al., 2012). The non-enveloped, triple-layered RV virion encapsidates an 11-segmented genome that encodes six structural (VP1-VP4, VP6, VP7) and six nonstructural (NSP1–NSP6) proteins (Desselberger, 2014). RV replicates primarily in mature enterocytes located at the villus tips of the small intestinal epithelium. Following attachment and endocytosis, RV sheds its outer layer (attachment protein VP4 and glycoprotein VP7) and releases a transcriptionally active double-layered particle (DLP) into the cytoplasm. The viral capping enzyme, VP3, modifies mRNAs with a 5′ cap as they are transcribed by the viral RNA-dependent RNA polymerase (RdRp), VP1, and extruded from the DLP. Capping by VP3 is incompletely efficient, which results in populations of uncapped and partially capped viral transcripts that activate host innate immune responses through the RNA-sensing PRRs RIG-I and melanoma differentiation-associated protein 5 (MDA5) (Broquet et al., 2011; Sen et al., 2011; Uzri and Greenberg, 2013). Genome replication and virion assembly are coordinated within cytoplasmic inclusions, or viroplasms, that likely serve to conceal dsRNA gene segments from detection by the host PRR machinery (Patton et al., 2006; Trask et al., 2012). Newly synthesized DLPs acquire their outer VP4/VP7 layer by budding through the endoplasmic reticulum, after which progeny virions exit the cell by lysis or exocytosis (Desselberger, 2014). Throughout the replication cycle, RV must contend with the host immune response. In this review, we discuss the structural and mechanistic basis of innate immune antagonism by two direct effectors, the RV NSP1 and VP3 proteins (Fig. 1).

Structure and function of RVA NSP1

The product of RV gene segment 5 is the nonstructural protein NSP1 (Desselberger, 2014). In RV species A (RVA), which is responsible for the majority of RV infection in humans, NSP1 is a ~57-kDa protein whose length ranges from 486 to 496 amino acids (Fig. 2A). NSP1 is the least conserved member of the RVA proteome, with sequence variability highest in the C-terminal half (Mitchell and Both, 1990). Phylogenetic analysis reveals that NSP1 sequences cluster according to host species (Dunn et al., 1994; Hua et al., 1993; Kojima et al., 1996); this indicates a possible role for NSP1 in host range restriction, which has been demonstrated in murine, but not other animal, models (Bridger et al., 1998; Ciarlet et al., 1998; Feng et al., 2011, 2013). An intact NSP1 protein is not essential for RV to propagate in permissive cell culture and a number of laboratory strains contain a rearranged gene 5 that encodes a C-terminally truncated NSP1 (Hua and Patton, 1994; Taniguchi et al., 1996; Tian

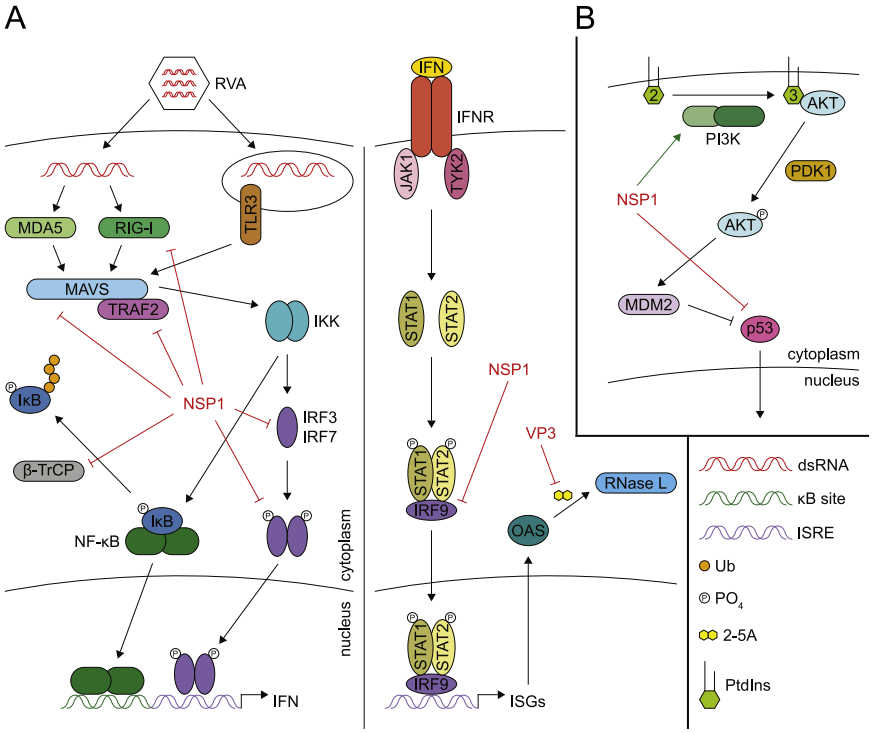

Fig. 1. Innate immune antagonism by RVA NSP1 and VP3. (A) Schematic of host innate immune responses to RV. Targets of RVA NSP1 and VP3 antagonist activity are indicated. (B) Schematic of the host PI3K/Akt pathway. Targets of RVA NSP1 activity are indicated.

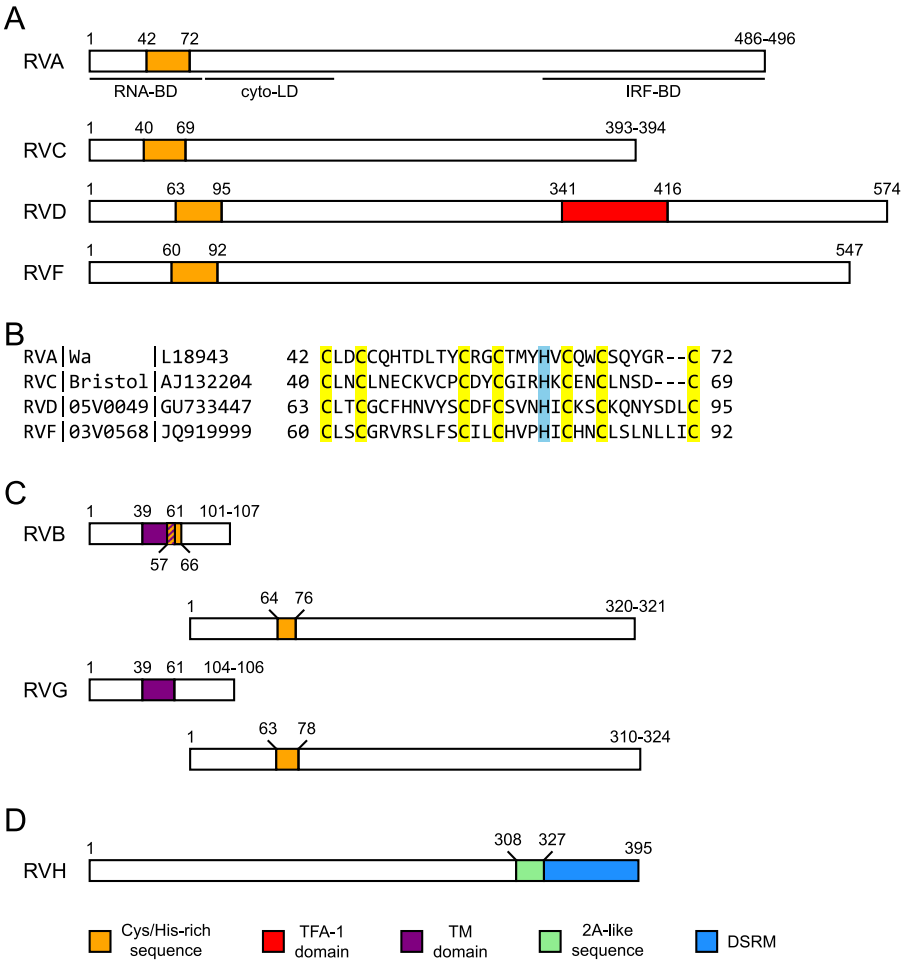

Fig. 2. Domain organization of RVA–RVH NSP1. (A) RVA-like NSP1 proteins contain a putative RING domain near the N terminus. RNA-BD, RNA-binding domain; cyto-LD, cytoskeleton localization domain; IRF-BD, IRF-binding domain. (B) Alignment of the putative RING domain of representative RVA-like NSP1 proteins. Conserved cysteine and histidine residues are colored yellow and blue, respectively. (C) RVB-like NSP1 proteins contain two overlapping ORFs. ORF1 and ORF2, respectively, contain a central TM domain and a short, N-terminal Cys/His-rich sequence. (D) RVH NSP1 contains a C-terminal 2A-like sequence and DSRM, like the NSP3 protein of RVC.

et al., 1993). Such strains can be generated by passage of parental (wild-type gene 5) strains at high multiplicity of infection (Hundley et al., 1985; Patton et al., 2001).

Despite significant sequence variability between NSP1 proteins, phylogenetic and biochemical analyses have identified key structural and functional domains. NSP1 contains a conserved zinc-binding, putative C_4-H-C_3 RING domain (consensus sequence: C-X_2-C-X_8-C-X_2-C-X_3-H-X-C-X_2-C-X_5-C) that spans residues 42–72 in most sequences (Brottier et al., 1992). The first 81 residues of simian SA11-4F NSP1, including the RING domain, mediate a specific interaction with the 5′ termini of viral mRNAs, which may prevent activation of cellular RNA sensors (Hua et al., 1994). SA11-4F NSP1 localizes to the cytoplasm during infection and associates with the cytoskeleton through a region that spans residues 84–176; deletion of this sequence results in NSP1 nuclear translocation (Hua et al., 1994; Hua and Patton, 1994). Through its variable C terminus, NSP1 interacts with a number of host proteins to induce their degradation (see below and Fig. 1)—typically, in a proteasome-dependent manner—and the conservation of an N-terminal RING domain strongly suggests that NSP1 functions as an E3 ubiquitin ligase (Graff et al., 2007). The RING domain is predicted to interact with a cellular E2 ubiquitin-conjugating enzyme, leading to polyubiquitination of the target protein bound at the NSP1 C terminus. However, difficulty in purifying recombinant NSP1 for use in ubiquitination assays has impeded confirmation of this activity.

Multilevel shutdown of the IFN response: NSP1-mediated degradation of IRFs

The interferon regulatory factor (IRF) family of transcription factors broadly influences cellular immune responses and is best known for its role in IFN induction (Savitsky et al., 2010). The nine mammalian IRFs (IRF1-IRF9) contain a conserved N-terminal DNA-binding domain (DBD) that recognizes IFN-stimulated response elements (ISREs) in the promoter region of IFN genes and ISGs. A C-terminal IRF association domain (IAD)—type 1 (IAD1) in IRF3-IRF9 and type 2 (IAD2) in IRF1/IRF2—mediates IRF homo- and hetero-dimerization and association with other transcription factors, including members of the STAT family. The IAD shares structural and electrostatic homology with the Forkhead-associated (FHA) and Mad homology 2 (MH2) domains found in a number of transcription factors (Qin et al., 2003). Activation signals from TLRs and RLRs induce IAD phosphorylation (IRF1, IRF3, IRF5, and IRF7 only) and/or dimerization, leading to IRF nuclear translocation and DBD binding to ISREs (Savitsky et al., 2010).

The first indication that NSP1 functions as an innate immune antagonist came from a yeast two-hybrid analysis that identified IRF3 as a cellular interaction partner of bovine B641 and murine EW NSP1 (Graff et al., 2002). Truncation of the NSP1 C terminus disrupts association with IRF3, although the N-terminal RING domain is also required. Subsequent work with simian RVA strains SA11-4F and SA11-30-19, along with variants (SA11-5S and

SA11-30-1A, respectively) that are isogenic except for a C-terminal truncation of NSP1 (17 and 71 residues, respectively), confirms the essential role of the C terminus in NSP1 function (Barro and Patton, 2005). Wild-type, but not C-terminally truncated, NSP1 suppresses nuclear translocation of IRF3 by inducing its proteasome-dependent turnover (Fig. 1A). SA11-5S and SA11-30-1A RVA induce a stronger IFN response and form smaller plaques than do their parent strains, indicating deficiencies in spread that likely result from impaired IFN antagonist activity by their NSP1 proteins. Disrupting the RING domain of B641 NSP1 abolishes interaction with, and degradation of, IRF3, providing the first evidence that NSP1 may function as an E3 ubiquitin ligase (Graff et al., 2007).

The overlap of mechanistic and structural features among members of the IRF family suggests that NSP1 might not simply mediate the degradation of IRF3 to block the IFN response. Indeed, IRF5 and IRF7 are targets of proteasome-dependent degradation by SA11-4F NSP1, but not the SA11-5S variant, indicating that NSP1 recognizes a conserved region within its targets (Fig. 1A) (Barro and Patton, 2007). Truncation of IRF3 has identified the IAD as the minimal domain necessary for degradation by SA11-4F NSP1 (Arnold et al., 2013a). The ability of NSP1 to mediate the degradation of IRF3, IRF5, and/or IRF7 is strain-specific and is most prevalent in NSP1 from animal strains (Arnold and Patton, 2011). In addition, SA11-4F and human Wa NSP1 induce the turnover of IRF9, but not of IRF1, suggesting that NSP1 only recognizes IAD1-containing IRFs (Fig. 1A) (Arnold et al., 2013a). IRF9, in response to type I/III IFN-mediated activation of the JAK-STAT pathway, assembles with STAT1 and STAT2 into the ISG factor 3 (ISGF3) complex, which translocates to the nucleus to bind ISREs and upregulate ISG expression (Fink and Grandvaux, 2013). Wa and simian RRV RVA inhibit nuclear translocation of STAT1 and STAT2, though NSP1 may not be required for this activity (Holloway et al., 2014, 2009). Further studies are required to assess whether NSP1 can also mediate the degradation of IRF4, IRF6, and IRF8, each of which contains a C-terminal IAD1.

Closing the door on NF-κB: NSP1-mediated degradation of β-TrCP and TRAF2

Like IRFs, the nuclear factor κB (NF-κB) family of transcription factors—p50, p52, p65, RelB, and c-Rel—plays a critical role in the induction of host immune responses (Hayden and Ghosh, 2012). An N-terminal Rel homology domain (RHD) mediates DNA binding and NF-κB homo- and heterodimerization, and a C-terminal transcription activation domain (TAD; present only in p65, RelB, and c-Rel) positively regulates target gene expression. NF-κB also broadly influences cell differentiation, proliferation, and survival, and its activation is therefore tightly regulated. In a resting cell, NF-κB dimers are held inactive in the cytoplasm by an associated inhibitor of κB (IκB) protein. Signals from PRRs and other molecules activate the IκB kinase (IKK) complex to phosphorylate IκB on a conserved degron motif (D$\underline{S}$GΦx$\underline{S}$; Φ, hydrophobic residue). This phosphodegron is recognized by β-transducin repeat containing protein (β-TrCP), a member of the F-box family of proteins that provides target specificity to the Skp-Cullin-F-box (SCF) family of E3 ubiquitin ligases. $SCF^{\beta\text{-TrCP}}$ induces the turnover of phosphorylated IκB, releasing NF-κB to translocate to the nucleus and bind κB sites in the promoter region of IFN genes and ISGs.

RVA NSP1 proteins do not universally conserve the ability to mediate IRF degradation (Arnold and Patton, 2011; Graff et al., 2007). Porcine OSU NSP1 potently blocks IFN-β induction during infection, despite having no effect on IRF3 turnover or nuclear translocation (Graff et al., 2009, 2007). Unlike the NSP1 proteins of most animal RVA strains, OSU NSP1 induces the proteasome-dependent degradation of β-TrCP (Fig. 1A) (Arnold and Patton, 2011; Graff et al., 2009). NF-κB activation is inhibited in both OSU-infected and OSU NSP1-transfected cells (Graff et al., 2009). In these cells, NSP1-mediated degradation of β-TrCP stabilizes IκBα (independent of phosphorylation status) and β-catenin, a target of β-TrCP that is central to the Wnt signaling pathway. Consequently, p65 does not translocate to the nucleus and p50 does not associate with DNA. Like OSU NSP1, bovine NCDV NSP1 targets β-TrCP for degradation and has similarly inhibitory effects on the NF-κB pathway, whereas the C-terminally truncated, bovine A5-16 NSP1 lacks these activities. Both OSU and NCDV NSP1 interact with β-TrCP, indicating that an association between NSP1 and target is likely necessary to induce turnover, as is true for NSP1 proteins that mediate IRF3 degradation.

Recently, microarray analysis of host gene expression in HT-29 (human colorectal adenocarcinoma) cells has demonstrated that infection with SA11-4F, Wa, or bovine A5-13 RVA upregulates transcription of the tumor necrosis factor (TNF)-α-induced protein 3 (TNFAIP3) gene (Bagchi et al., 2012). TNFAIP3, or A20, is a zinc-finger protein that inhibits NF-κB activation in response to numerous stimuli, including PRRs (Catrysse et al., 2014). Treatment of RV-infected cells with A20 siRNA reduces viral titer 10–100 fold (Bagchi et al., 2013a). In addition, infection with A5-13, but not A5-16, RVA induces the NSP1-mediated and proteasome-dependent degradation of TNF receptor-associated factor 2 (TRAF2), a target of A20 activity (Fig. 1A). TRAF molecules are involved in mediating signals from a number of cellular receptors, including those that activate NF-κB (Xie, 2013). A region of NSP1 between residue 101 and the C terminus, which excludes the N-terminal RING domain, mediates interaction with TRAF2 (Bagchi et al., 2013a). Turnover of TRAF2 inhibits p52 nuclear translocation, thereby arresting NF-κB activation.

No dsRNA here: NSP1-mediated degradation of RIG-I and MAVS

Nucleic acids make up the largest class of PAMPs detected by host PRRs (Reikine et al., 2014). Members of the RLR family—RIG-I, MDA5, and laboratory of genetics and physiology 2 (LGP2)—sense cytoplasmic dsRNA through a conserved DExD/H-box helicase and C-terminal domain (CTD). RIG-I recognizes 5′-triphosphorylated blunt ends of short (<300 bp) dsRNA, whereas MDA5 lacks end specificity and binds to internal sites on long (>1000 bp) dsRNA (Hornung et al., 2006; Kato et al., 2006; Pichlmair et al., 2006). Upon dsRNA binding, N-terminal caspase recruitment domains (CARDs) in RIG-I and MDA5 mediate oligomerization and association with mitochondrial antiviral signaling protein (MAVS), ultimately resulting in activation of IRFs and NF-κB (Reikine et al., 2014). Although LGP2 also recognizes dsRNA ends, it lacks CARD domains and cannot signal through MAVS; instead, LGP2 acts as a positive and negative regulator of MDA5 and RIG-I function, respectively.

SA11-4F and bovine UK NSP1 can block IRF3 transcriptional activity without inducing its turnover, suggesting that another mechanism is involved (Qin et al., 2011; Sen et al., 2009). A study with OSU and SA11-4F NSP1, including a deletion mutant of SA11-4F that lacks the C-terminal IRF-binding region, demonstrates that NSP1 can block RIG-I-mediated activation of IFN-β (Fig. 1A) (Qin et al., 2011). All three NSP1 proteins associate with RIG-I, though it is not known whether RNA bridges this interaction. Surprisingly, OSU and SA11-4F NSP1 induce the proteasome-independent turnover of RIG-I, without affecting the level of RIG-I mRNA transcripts. However, multiple NSP1 proteins—A5-13, human DS-1, EW, human KU, OSU, RRV, and SA11-4F—target MAVS for degradation in a proteasome-dependent manner (Nandi et al., 2014). SA11-4F NSP1, through its C-terminal 100 residues and independent of the RING domain, interacts with the CARD and/or transmembrane (TM) domains of MAVS. Unlike its full-length counterparts, A5-16 NSP1 fails to block the formation of MAVS aggregates and the concomitant induction of IFN-β, confirming the role of the NSP1 C terminus in antagonizing MAVS. Together, these

data indicate that NSP1 can block innate immune signaling at both the transcriptional (IRF, NF-κB) and PRR level. Future work to characterize the interactions of NSP1 with RIG-I and MAVS may reveal effects that NSP1 has on MDA5 and LGP2 activity and turnover.

Keeping the lights on: NSP1-mediated activation of PI3K/Akt and degradation of p53

Viruses are obligate intracellular parasites that rely on host machinery to propagate. A key host defense mechanism is the induction of apoptosis in infected cells, which limits viral spread and prevents further host pathogenesis (Diehl and Schaal, 2013). A number of viruses circumvent apoptosis by interfering with the phosphoinositide 3-kinase (PI3K)/Akt signaling pathway. Class I PI3Ks, the best-characterized members of the PI3K family, are composed of a catalytic p110 subunit and a regulatory p85 subunit, of which two isomers (p85α and p85β) commonly interact with viral proteins (Bagchi et al., 2013b; Diehl and Schaal, 2013). Signals from cytokine and other growth factor receptors activate PI3K, which phosphorylates the lipid substrate phosphatidylinositol (PtdIns) to generate PtdIns-3,4,5-triphosphate (PIP_3) (Diehl and Schaal, 2013). The serine/threonine kinase Akt recognizes PIP_3 and undergoes activating phosphorylation by phosphoinositide-dependent kinase 1 (PDK1). Akt then signals to activate cellular factors related to translation and growth and to inhibit apoptotic factors.

Recent studies show that A5-13, but not A5-16, RVA activates the PI3K/Akt pathway to prevent premature apoptosis (Fig. 1B) (Bagchi et al., 2010, 2013b). Unlike A5-16, A5-13 infection induces rapid and long-lived phosphorylation of Akt and one of its substrates, glycogen synthase kinase 3β (GSK3β) (Bagchi et al., 2010). This ultimately results in delayed apoptosis, as indicated by upregulated expression of X-linked inhibitor of apoptosis (XIAP) and delayed cleavage of caspase 3 and poly(ADP-ribose) polymerase (PARP) in cells infected with A5-13, but not A5-16. These effects are mediated by NSP1 and depend on sustained activation of NF-κB, but do not require IFN. Treatment with PI3K or NF-κB inhibitors attenuates A5-13 growth by nearly 100 fold. A5-13, but not A5-16, NSP1 interacts with the p85 subunit of PI3K, indicating that the C-terminal region of NSP1 is likely required for this association. The p85 protein contains four Src-homology (SH) domains: an N-terminal SH3 domain and an inter-SH2 (iSH2) domain that interacts with p110 and is bracketed by two additional SH2 domains (Yu et al., 1998). Deletion mutagenesis indicates that NSP1 binds the SH3 domain of p85α and the three SH2 domains of p85β (Bagchi et al., 2013b). Both N- and C-terminal fragments of NSP1 can interact with p85α, but p85β preferentially associates with full-length NSP1. Since the PI3K/Akt pathway also induces ISG expression, the innate immune antagonist functions of NSP1 likely serve to neutralize this effect (Diehl and Schaal, 2013).

Among the targets of PI3K/Akt activity is p53, a stress-responsive transcription factor that plays a significant role in apoptosis, cell cycle regulation, and other processes (Rivas et al., 2010). In an unstressed cell, the E3 ubiquitin ligase mouse double minute 2 homolog (MDM2) targets hypophosphorylated p53 for degradation. Stress signals induce p53 phosphorylation to block MDM2-mediated turnover, leading to nuclear translocation of p53 and upregulation of target gene expression. Infection of cells with SA11-4F, but not A5-16, RVA results in the posttranscriptional depletion of p53, suggesting that NSP1 mediates this activity (Bhowmick et al., 2013). Indeed, expression of full-length, but not C-terminally truncated, NSP1 induces the proteasome-dependent degradation of p53; inhibitors of PI3K and MDM2 do not arrest this turnover (Fig. 1B). Infection with SA11-4F, but not A5-16, delays upregulation of p53-upregulated modulator of apoptosis (PUMA) and mitochondrial translocation of Bax—two downstream effectors of p53-induced apoptotic pathways—and occurs independently of PI3K activation (Bhowmick et al., 2013; Rivas et al., 2010). NSP1 interacts with the DBD (residues 100–300) of p53 through a region C-terminal to the RING domain (Bhowmick et al., 2013). As expected, the RING domain is required to induce p53 turnover.

Structure and function of non-RVA NSP1

RVs have been divided into eight species (RVA–RVH) based on the sequence of gene segment 6, which encodes the intermediate capsid protein, VP6 (Matthijnssens et al., 2012). All RV species infect animals, though only RVA–RVC and RVH are currently known to infect humans (Ghosh et al., 2010; Jiang et al., 2008; Soma et al., 2013). In humans, RVH has been found only in adults, whereas RVA–RVC have been found in both adults and children. RVD, RVF, and RVG have been isolated exclusively from avian species (Kindler et al., 2013; Phan et al., 2013; Trojnar et al., 2010). Although comparatively few non-RVA NSP1 sequences are available, intra- and interspecies alignments suggest that NSP1 proteins form three functional classes: RVA-like (RVA, RVC, RVD, RVF), RVB-like (RVB, RVG), and RVH (Fig. 2).

RVA-like NSP1 proteins share an N-terminal, putative RING domain (consensus sequence: C-X_2-C-X_8-C-X_2-C-X_3-H-X-C-X_2-C-X_{4-7}-C); the only difference is the length of the spacer (4–7 amino acids) between the final pair of cysteine residues (Fig. 2A and B). However, aside from RVA NSP1, it is not known if these proteins mediate the degradation of cellular factors (Fig. 1). RVA NSP1 is most closely related to its substantially shorter RVC counterpart (486–496 *versus* 393–394 residues) (Hua et al., 1993). RVD NSP1 (574 residues) is most homologous to avian RVA NSP1; the low sequence identity between avian and mammalian RVA NSP1 may indicate a past reassortment event between RVD and avian RVA NSP1 (Ito et al., 2001; Trojnar et al., 2009). RVD and avian RVA NSP1 conserve a domain of the transcription initiation factor IIE alpha subunit (TFA-1) superfamily (19–35% amino acid identity) that spans residues 341–416 in RVD NSP1 (Trojnar et al., 2010). RVF NSP1 (547 residues) shares partial sequence homology with the N-terminal half of RVD and avian RVA NSP1 (Kindler et al., 2013).

The gene encoding RVB-like NSP1 contains two overlapping open reading frames (ORFs; Fig. 2B); this is similar to RVA gene segment 11, which encodes the nonstructural proteins NSP5 and NSP6 (Desselberger, 2014; Ghosh et al., 2010; Kindler et al., 2013; Phan et al., 2013). The RVB ORF2 product has been detected more consistently than the ORF1 product in *in vitro* translation systems and is also recognized by immune serum of RVB-infected rats, indicating that the ORF2 protein is produced during infection (Eiden, 1994; Shen et al., 1999). RVB NSP1 sequences cluster according to host species, which suggests a role for NSP1 in RVB host range restriction (Ghosh et al., 2010). The protein encoded by ORF1 (RVB, 101–107 residues; RVG, 104–106 residues) does not contain any obvious structural features, but does contain a hydrophobic/nonpolar sequence (residues 39–61) that may be a TM domain; in RVB NSP1, this region also overlaps with a short, Cys-rich sequence (residues 57–66) (Kobayashi et al., 2001). The ORF2 protein (RVB, 320–321 residues; RVG, 310–324 residues) contains a short, Cys/His-rich sequence near the N terminus (RVB, residues 64–76; RVG, residues 63–78). A few RVB isolates contain a putative ORF3, but this ORF varies significantly in length (65–146 residues) and lacks any distinguishing features.

RVH NSP1 (395 residues) is most closely related to ORF2 of RVB NSP1 and contains a C-terminal dsRNA-binding motif (DSRM; residues 327–395) that immediately follows a picornavirus 2A-like sequence (Fig. 2C) (Yang et al., 2004). The 2A-like sequence terminates in an NPGP motif that induces a ribosomal skip between the glycine and second proline residues to produce two polypeptides (Donnelly et al., 2001a, 2001b). The NSP3 protein of RVC also contains a C-terminal DSRM preceded by a 2A-like sequence; RVC NSP3 is

'cleaved' into two polypeptides and the DSRM prevents activation of the ISG protein kinase R (PKR) by binding to dsRNA (Langland et al., 1994). Presumably, the DSRM of RVH NSP1 functions in the same manner, since there are no obvious Cys/His-rich sequences in the N-terminal region that might function as a RING domain.

Structure and function of RVA VP3

The product of RV gene segment 3 is the structural protein VP3 (Desselberger, 2014). RVA VP3 is an 835-residue, ~98-kDa protein that is packaged into virions in low copy number. Using reassortant genetics, VP3 has been linked to species-specific virulence properties in mouse and piglet models of infection, suggesting a potential role in host range restriction (Feng et al., 2013; Hoshino et al., 1995; Wang et al., 2011). Studies with purified RV subviral particles demonstrate that VP3 has biochemical properties consistent with those of RNA capping enzymes. First, VP3 binds single-stranded RNA (ssRNA), with a preference for capped species (Patton and Chen, 1999). Second, VP3 binds covalently and reversibly to GMP and can transfer this moiety to pyrophosphate or GDP, which is consistent with guanylyltransferase (GT) activity (Fukuhara et al., 1989; Liu et al., 1992; Pizarro et al., 1991). Finally, RV subviral particles can produce methylated caps *in vitro* in the presence of S-adenosyl-L-methionine (SAM); in these particles, VP3 can be chemically cross-linked to SAM, which is consistent with SAM-dependent methyltransferase (MT) activity (Chen et al., 1999; Spencer and Garcia, 1984). Despite incomplete capping and methylation efficiency (Imai et al., 1983; Uzri and Greenberg, 2013), modification by VP3 may help prevent the detection of RV mRNAs by cellular innate immune molecules, including RIG-I, which recognizes 5′-triphosphorylated RNA, and IFN-induced protein with tetratricopeptide repeats 1 (IFIT1), which recognizes and inhibits translation of mRNAs that lack 2′-O-methylation (Daffis et al., 2010; Hornung et al., 2006; Pichlmair et al., 2006). In addition to its capping activities, RVA VP3 has been shown to cleave 2′,5′-oligoadenylates (2-5As), signaling molecules produced by the cytoplasmic dsRNA sensor oligoadenylate synthetase (OAS) that activate the latent ribonuclease (RNase L) to cleave single-stranded viral and cellular RNAs (Silverman, 2007; Silverman and Weiss, 2014; Zhang et al., 2013). RNA fragments produced by RNase L reduce viral replication by activating RLRs to amplify IFN production and by inducing apoptosis to eliminate infected cells. Thus, the multifunctional RVA VP3 protein may contribute to innate immune evasion and virulence by indirect (viral mRNA capping) and direct (2-5A cleavage) mechanisms.

Understanding the molecular basis of these activities has been limited by a dearth of structural information for VP3, difficulties in purifying the recombinant protein, and the lack of an RV reverse genetics system. Key insights have been provided by homology modeling with a number of reported structural homologs of VP3: the capping enzymes of fellow *Reoviridae* member bluetongue virus (BTV VP4; VP3 residues 39–634), vaccinia virus (VACV VP39; VP3 residues 257–333), and members of the 2H phosphoesterase superfamily, including the cellular A kinase anchoring protein 7 (AKAP7; VP3 residues 697–800) (Gold et al., 2008; Hodel et al., 1996; Ogden et al., 2014; Sutton et al., 2007; Zhang et al., 2013). RVA VP3 is predicted to contain five structurally distinct domains: an N-terminal domain (NTD) of unknown function; a guanine-N7-MT with an inserted 2′-O-MT; a combined RNA 5′-triphosphatase (RTP)/GT; and a C-terminal 2′,5′-phosphodiesterase (PDE) (Ogden et al., 2014; Zhang et al., 2013).

Capping domains of RVA VP3

Like BTV VP4, the N-terminal ~700 amino acids of RVA VP3 are predicted to form a capping assembly line (Fig. 3A) (Ogden et al., 2014; Sutton et al., 2007). The VP3 NTD (the N-terminal ~175 residues) is thought to contain a kinase-like fold that, like the NTD of BTV VP4, lacks the catalytic residues and P-loop required for kinase activity. While no functional data for the VP3 NTD have been reported, the corresponding domain of BTV VP4 is proposed to act as an adaptor that bridges interactions with the viral RdRp.

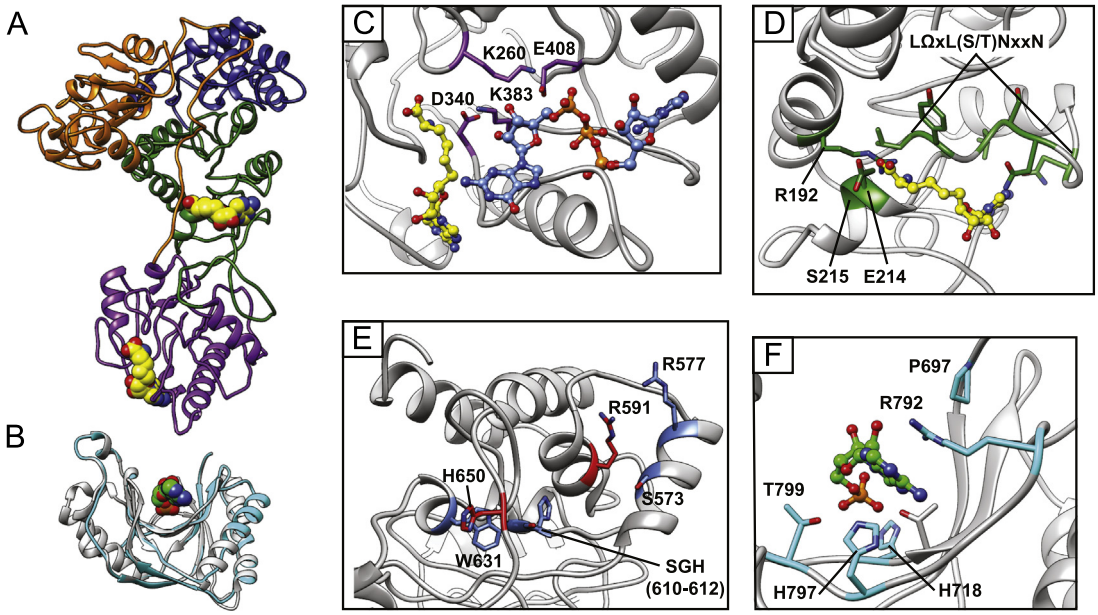

Fig. 3. Predicted structure and active sites of RVA VP3. (A) Capping region (residues 1–688) of RVA RRV VP3, colored by domain (Ogden et al., 2014). Orange, NTD; green, N7-MT; purple, 2′-O-MT; blue, RTP/GT. (B) 2′,5′-PDE domain (cyan; residues 695–835) of RVA SA11 VP3 overlaid on the central domain of AKAP7 (Gold et al., 2008; Zhang et al., 2013). (C) 2′-O-MT domain. Predicted KDKE motif residues are shown. (D) N7-MT domain. R192 and conserved residues in the GxxxE(S/T) and LΩxL(ST)NxxN motifs are shown. (E) RTP/GT domain. Blue, residues strictly conserved in sequence alignments of RV VP3 and orbivirus VP4; red, residues required for autoguanylation. (F) 2′,5′-PDE domain. Residues that are strictly conserved in sequence alignments of RV VP3, coronavirus ns2, and AKAP7 are shown. Ligands (yellow, SAH; light blue, cap analog) from structures of BTV VP4 (PDB ID: 2JHP, 2JHA) are overlaid in panels A, C, and D. Ligand (green, AMP) from a structure of the AKAP7 central domain (PDB ID: 2VFK) is overlaid in panels B and F.

The canonical class I, SAM-dependent MT fold is a seven-stranded β-sheet that is flanked on either side by three α-helical regions, though there is limited sequence identity among these enzymes (Decroly et al., 2012). N7-MTs are thought to catalyze methylation through optimal substrate positioning and electrostatic environment, whereas 2′-O-MTs employ a conserved, catalytic KDKE tetrad, with the second lysine playing a prominent role in catalysis. The identification of RVA VP3 residues ~250–440 as the 2′-O-MT domain is supported primarily by predicted homology with the 2′-O-MT domains of BTV VP4 and VACV VP39 (Ogden et al., 2014). Although some discrepancy exists in the precise identity of the VP3 residues that are predicted to form the KDKE tetrad, homology models place these residues in a conformation consistent with catalytic function (Fig. 3A and C). Predictions regarding the disrupted N7-MT domain of RVA VP3 (residues ~175–250 and 440–555) are rooted in the noteworthy conservation of sequences that form the major SAM-binding surface in the corresponding domain of BTV VP4 (Ogden et al., 2014). These amino acids include R192, a GxxxE(S/T) motif that spans residues 134–139, and an LΩxL(S/T)NxxN motif that spans residues 409–417 (Ω, aromatic residue; Fig. 3D) (Kindler et al., 2013; Ogden et al., 2014). Biochemical confirmation of the 2′-O- and N7-MT domain and residue assignments is currently lacking.

RVA VP3 residues ~555–690 are proposed to form an α-helical RTP/GT domain (Fig. 3A) (Ogden et al., 2014). The homologous domain in BTV VP4 covalently binds GMP *in vitro* and forms a six-helix bundle, a structural arrangement not previously observed for an RTP or GT (Sutton et al., 2007). While recombinant BTV VP4 has demonstrated nucleoside 5′-triphosphatase activity *in vitro*, assignment of the CTD as the RTP is based solely on the presence of a conserved cysteine at the base of a depression, in the context of sequences reminiscent of a cysteine phosphatase HCxxxxxR motif; this cysteine is not conserved in RVA VP3 (Ogden et al., 2014; Sutton et al., 2007; Takagi et al., 1997). Thus, the identity of the RTP domain remains an open question for both RVs and orbiviruses. Sequence alignment of RV and orbivirus GT domains reveals strict conservation at RVA VP3 positions S573, R577, W631, and H650, and within an SGHΦ motif that spans residues 552–555 (Fig. 3E) (Ogden et al., 2014). Autoguanylation assays with recombinant RVA VP3 proteins mutagenized at conserved lysine, arginine, and histidine residues within the predicted GT domain provide biochemical support for its assigned function and identify residues R591 and H650 as candidate sites of autoguanylation. Although their precise positions differ between RVA VP3 structural models, the conserved and potentially catalytic residues occupy adjacent, surface-exposed regions within loops and a depression in the GT domain and likely contribute to folding, ligand binding, and catalysis. In particular, the exquisite conservation of the SGHΦ motif within the RTP/GT domain of RV and orbivirus capping enzymes suggests a functional role, but the mechanisms of RTP and GT activity remain to be determined.

Still no dsRNA here: antagonism of OAS/RNase L by the 2′,5′-PDE domain of VP3

Support for homology of the C-terminal ~140 residues of RVA VP3 with the central domain of AKAP7 comes from studies using computational, biochemical, and biological methods. Both sequence analysis and homology modeling predict that the CTD of RVA VP3 is homologous with 2H phosphoesterase superfamily proteins (Mazumder et al., 2002; Zhang et al., 2013). The conserved fold of these proteins consists of a central, concave β-sheet that is flanked below by two β-strands and on either side by two α-helical regions (Mazumder et al., 2002). Two HΦ(S/T)Φ motifs sit at the base of the groove formed by the concave β-sheet; the histidine and threonine residues are proposed to be involved in catalysis and substrate stabilization, respectively. The central domain of AKAP7 adopts a similar fold and, in complex with AMP, served as the basis for a structural model of the RVA VP3 CTD (Gold et al., 2008; Zhang et al., 2013). The VP3 model contains a central, concave structure of β-strands and loops, with two β-strands running underneath; the HΦ(S/T)Φ motifs overlay very closely with those of AKAP7 and are positioned to interact with AMP in a similar manner (Fig. 3B). However, the central sheet in the VP3 model appears to lack some of the β-strands present in AKAP7, and at least one of the α-helical regions appears to have been replaced with a loop. Since the CTD of RVA VP3 is ~50 residues shorter than the central domain of AKAP7, it is likely that at least some of their structural features will differ.

Phylogenetic analysis indicates that RVA VP3, AKAP7, and the ns2 protein of betacoronaviruses, including the model murine pathogen mouse hepatitis virus (MHV), belong to the eukaryotic-viral LigT-like group of the 2H phosphoesterase superfamily (Mazumder et al., 2002). Each of these proteins has been shown to possess 2′,5′-PDE activity and can cleave 2-5A *in vitro* to antagonize RNase L, which supports the predicted homology between VP3 CTD and AKAP7 (Gusho et al., 2014; Zhang et al., 2013; Zhao et al., 2012). While the significance of 2′,5′-PDE activity remains to be determined for RV, studies using recombinant MHV that expresses wild-type or catalytically inactive ns2 have demonstrated that this activity is required for efficient viral replication in some cell types (primarily macrophages) and for pathogenesis in mice (Zhao et al., 2012). In *trans* expression of the RVA VP3 CTD in the genome of MHV that encodes an inactive ns2 protein confers near wild-type levels of viral growth and pathogenesis in infected mice, which suggests that the 2′,5′-PDE activity of RVA VP3 is present and relevant in a biological context (Zhang et al., 2013). Mutating either of the predicted catalytic histidine residues results in a loss of catalytic activity and of the capacity to complement inactive ns2, providing further support for the AKAP7-based homology model (Banerjee et al., 2014; Zhang et al., 2013). In alignments of the RVA VP3 CTD, coronavirus ns2, torovirus polyprotein 1ab, and AKAP7, the only residues that are conserved across all sequences, aside from both catalytic histidine residues and threonine residue in the second HΦ(S/T)Φ motif, are P697 and R792 in RVA VP3 (Zhang et al., 2013). The AKAP7 residue that corresponds to R792 in RVA VP3 is located on the 'R-loop' and forms a π–π stack with bound AMP (Gold et al., 2008). R792 is located on a related loop in RVA VP3, adjacent to P697 and oriented appropriately to form a similar interaction with AMP in the modeled structure (Fig. 3F) (Zhang et al., 2013). While the mechanism of specific 2-5A recognition by 2H superfamily 2′,5′-PDEs remains to be determined, these observations suggest that the conserved proline and 'R-loop' arginine residues may be involved.

Structure and function of non-RVA VP3

Modeling studies and sequence comparisons have suggested differences in the domain organization of VP3 from other RV species (Ogden et al., 2014). RVB and RVG VP3 sequences contain an insertion in the predicted N7-MT domain that is shorter than the predicted 2′-O-MT domain of the other species. Accordingly, a central region of VP3 from all species but RVB and RVG is predicted with high confidence to be homologous to VACV VP39. Like RVA VP3, RVB and RVG VP3 contains a CTD that extends beyond the predicted capping region and that may function as a 2′,5′-PDE, based on predicted homology to AKAP7—albeit with less confidence than for RVA VP3—and the apparent conservation of HΦ(S/T)Φ motifs (Mazumder et al., 2002; Ogden et al., 2014; Zhang et al., 2013). However, a polymorphism in the second HΦ(S/T)Φ motif of RVG VP3 may preclude catalytic activity. While predicted

differences in the 2′-O-MTase and 2′,5′-PDE domains of VP3 may result in differential capacity to evade the antiviral effects of IFITs and the OAS/RNase L pathway, differences in host species or pathobiology may render these effects more or less important for different RV species, in terms of viral fitness.

VP3 function in the context of RV particles

Structural and biochemical studies have begun to shed light on the incompletely understood interactions between RdRp VP1, inner capsid protein VP2, and VP3 that mediate packaging, replication, and transcription. Encapsidation assays with recombinantly expressed RV structural proteins have shown that, although VP3 incorporation into RV-like particles does not depend upon VP1, it requires the flexible N-terminal arms of VP2 that approach the icosahedral fivefold vertices in the particle interior (McClain et al., 2010; Zeng et al., 1998). Cryo-electron microscopy image reconstructions of RV-like particles with *versus* without encapsidated VP1 and VP3 suggest that both molecules sit at the fivefold vertices, though only the orientation of VP1 has been resolved unambiguously (Estrozi et al., 2013; Prasad et al., 1996). Viral mRNA and dsRNA are hypothesized to emerge from separate tunnels of the four-tunneled VP1 (Lu et al., 2008). To orient VP3 appropriately for interaction with nascent mRNAs during transcription, the GTase domain would be expected to sit proximal to the mRNA exit tunnel of VP1. However, placement of VP1 with its putative mRNA exit tunnel directly adjacent to a channel in the VP2 layer leaves little room for VP3 to intervene between mRNA synthesis and extrusion from the particle (Estrozi et al., 2013). This observation suggests that VP1 adopts a distinct orientation in resting *versus* active RV DLPs, an idea that is indirectly supported by the structural homogeneity of these particles in solution (Gilmore et al., 2013). Alternatively, VP1 positioning within virions or inefficient VP3 encapsidation may, in part, explain the incomplete efficiency of RV mRNA capping and methylation (Imai et al., 1983; Uzri and Greenberg, 2013).

VP3-mediated host range restriction

The mechanisms by which RVA VP3 mediates host range restriction remain unclear. The ssRNA-binding activity of RVA VP3 is fairly nonspecific and other known substrates, including SAM, GTP, and 2-5A, are universal across different species. However, basal levels of OAS and RNase L differ based on cell type, with higher levels detected in murine macrophages *versus* fibroblasts (Banerjee et al., 2014). Differences in VP3 enzymatic efficiency and interactions with other viral proteins may explain the host-specific virulence effects observed for reassortant viruses in animal models, but an apparent lack of difference in infectivity for most of these viruses *in vitro* is more consistent with innate immune-mediated effects (Feng et al., 2013; Hoshino et al., 1995; Wang et al., 2011). Although VP3 has been classified as a structural protein and is known to perform capping functions in the context of subviral particles, the cytoplasmic localization of OAS, RNase L, and 2-5A suggests that VP3 may also function independently of the particle and engage in specific interactions with host proteins. Analysis of a small number of RVA VP3 sequences has identified three host-specific motifs (residues 197–207, 452–456, and 637–642) (Subodh et al., 2006). In a homology model of the RVA VP3 capping region (Fig. 3A), these motifs correspond to two loops on the side of the N7-MT domain opposite the catalytic site and to a helix in the RTP/GT domain; these are regions of low conservation among clade A VP3 sequences and, therefore, are candidate sites for species-specific protein interactions (Ogden et al., 2014).

Indirect antagonism of the host immune response by RVA

A virus must continually defend itself against the onslaught of host immune responses that serve to arrest infection at all stages of the viral life cycle, and RV is equipped with a number of indirect defenses not covered in this review (Arnold et al., 2013b; Desselberger, 2014). RV enters the cytoplasm as a transcriptionally active, closed particle that shields the viral dsRNA genome from detection by host PRRs. Expression of the NSP3 protein, which binds both eukaryotic translation initiation factor 4G (eIF4G) and the 3′ consensus sequence of viral transcripts, skews host translation to favor viral mRNAs and disrupts nuclear-cytoplasmic transport of poly(A)-binding protein (PABP); this has the added benefit of suppressing translation of the host proteins that are required to mount an antiviral response. Other viral proteins that bind dsRNA, including NSP6 and the DSRM encoded by some non-RVA species, likely serve as added layers of protection against PRRs and other cellular sensors. Finally, sequestration of the viral replication machinery in dense viroplasms, and coordination of genome replication and particle assembly, shield newly synthesized RV RNAs from host sensors.

Conclusions

The structural and mechanistic properties of NSP1 and VP3 allow these proteins to directly antagonize host innate immune responses. NSP1 is a putative E3 ubiquitin ligase that mediates the degradation of a wide range of cellular targets, including those that function as innate immune sensors (RIG-I), signaling intermediates (TRAF2, MAVS, and β-TrCP), transcription factors (IRFs), and mediators of host survival pathways (PI3K and p53). In many respects, VP3 is two proteins in one: it caps viral transcripts as they emerge from RV DLPs, which likely prevents activation of host RNA sensors, and it directly antagonizes the dsRNA-responsive OAS/RNase L pathway by cleaving the signaling molecule 2-5A. VP3 may also function in two distinct regions of the cell during infection: within a viral particle as the capping enzyme and perhaps also within the cytoplasm as a direct innate immune antagonist. The varied functions of NSP1 and VP3 highlight the diversity and importance of cellular innate immune defenses to RNA viruses and likely reflect the requisite compactness of a viral genome.

Acknowledgments

This work was supported by the Intramural Research Program of the National Institute of Allergy and Infectious Diseases at the National Institutes of Health (Z1A AI000754 and Z1A AI000788).

References

Arnold, M.M., Barro, M., Patton, J.T., 2013a. Rotavirus NSP1 mediates degradation of interferon regulatory factors through targeting of the dimerization domain. J. Virol. 87, 9813–9821.

Arnold, M.M., Patton, J.T., 2011. Diversity of interferon antagonist activities mediated by NSP1 proteins of different rotavirus strains. J. Virol. 85, 1970–1979.

Arnold, M.M., Sen, A., Greenberg, H.B., Patton, J.T., 2013b. The battle between rotavirus and its host for control of the interferon signaling pathway. PLoS Pathog. 9, e1003064.

Bagchi, P., Bhowmick, R., Nandi, S., Kant Nayak, M., Chawla-Sarkar, M., 2013a. Rotavirus NSP1 inhibits interferon induced non-canonical NFkappaB activation by interacting with TNF receptor associated factor 2. Virology 444, 41–44.

Bagchi, P., Dutta, D., Chattopadhyay, S., Mukherjee, A., Halder, U.C., Sarkar, S., Kobayashi, N., Komoto, S., Taniguchi, K., Chawla-Sarkar, M., 2010. Rotavirus nonstructural protein 1 suppresses virus-induced cellular apoptosis to facilitate viral growth by activating the cell survival pathways during early stages of infection. J. Virol. 84, 6834–6845.

Bagchi, P., Nandi, S., Chattopadhyay, S., Bhowmick, R., Halder, U.C., Nayak, M.K., Kobayashi, N., Chawla-Sarkar, M., 2012. Identification of common human host

genes involved in pathogenesis of different rotavirus strains: an attempt to recognize probable antiviral targets. Virus Res. 169, 144–153.
Bagchi, P., Nandi, S., Nayak, M.K., Chawla-Sarkar, M., 2013b. Molecular mechanism behind rotavirus NSP1-mediated PI3 kinase activation: interaction between NSP1 and the p85 subunit of PI3 kinase. J. Virol. 87, 2358–2362.
Banerjee, S., Chakrabarti, A., Jha, B.K., Weiss, S.R., Silverman, R.H., 2014. Cell-type-specific effects of RNase L on viral induction of beta interferon. mBio 5, e00856–00814.
Barro, M., Patton, J.T., 2005. Rotavirus nonstructural protein 1 subverts innate immune response by inducing degradation of IFN regulatory factor 3. Proc. Natl. Acad. Sci. USA 102, 4114–4119.
Barro, M., Patton, J.T., 2007. Rotavirus NSP1 inhibits expression of type I interferon by antagonizing the function of interferon regulatory factors IRF3, IRF5, and IRF7. J. Virol. 81, 4473–4481.
Bhowmick, R., Halder, U.C., Chattopadhyay, S., Nayak, M.K., Chawla-Sarkar, M., 2013. Rotavirus-encoded nonstructural protein 1 modulates cellular apoptotic machinery by targeting tumor suppressor protein p53. J. Virol. 87, 6840–6850.
Bridger, J.C., Dhaliwal, W., Adamson, M.J., Howard, C.R., 1998. Determinants of rotavirus host range restriction – a heterologous bovine NSP1 gene does not affect replication kinetics in the pig. Virology 245, 47–52.
Broquet, A.H., Hirata, Y., McAllister, C.S., Kagnoff, M.F., 2011. RIG-I/MDA5/MAVS are required to signal a protective IFN response in rotavirus-infected intestinal epithelium. J. Immunol. 186, 1618–1626.
Brottier, P., Nandi, P., Bremont, M., Cohen, J., 1992. Bovine rotavirus segment 5 protein expressed in the baculovirus system interacts with zinc and RNA. J. Gen. Virol. 73, 1931–1938.
Catrysse, L., Vereecke, L., Beyaert, R., van Loo, G., 2014. A20 in inflammation and autoimmunity. Trends Immunol. 35, 22–31.
Chen, D., Luongo, C.L., Nibert, M.L., Patton, J.T., 1999. Rotavirus open cores catalyze 5′-capping and methylation of exogenous RNA: evidence that VP3 is a methyltransferase. Virology 265, 120–130.
Ciarlet, M., Estes, M.K., Barone, C., Ramig, R.F., Conner, M.E., 1998. Analysis of host range restriction determinants in the rabbit model: comparison of homologous and heterologous rotavirus infections. J. Virol. 72, 2341–2351.
Daffis, S., Szretter, K.J., Schriewer, J., Li, J., Youn, S., Errett, J., Lin, T.Y., Schneller, S., Zust, R., Dong, H., Thiel, V., Sen, G.C., Fensterl, V., Klimstra, W.B., Pierson, T.C., Buller, R.M., Gale Jr., M., Shi, P.Y., Diamond, M.S., 2010. 2′-O methylation of the viral mRNA cap evades host restriction by IFIT family members. Nature 468, 452–456.
Decroly, E., Ferron, F., Lescar, J., Canard, B., 2012. Conventional and unconventional mechanisms for capping viral mRNA. Nat. Rev. Microbiol. 10, 51–65.
Desselberger, U., 2014. Rotaviruses. Virus Res. 190, 75–96.
Diehl, N., Schaal, H., 2013. Make yourself at home: viral hijacking of the PI3K/Akt signaling pathway. Viruses 5, 3192–3212.
Donnelly, M.L., Hughes, L.E., Luke, G., Mendoza, H., ten Dam, E., Gani, D., Ryan, M.D., 2001a. The 'cleavage' activities of foot-and-mouth disease virus 2A site-directed mutants and naturally occurring '2A-like' sequences. J. Gen. Virol. 82, 1027–1041.
Donnelly, M.L., Luke, G., Mehrotra, A., Li, X., Hughes, L.E., Gani, D., Ryan, M.D., 2001b. Analysis of the aphthovirus 2A/2B polyprotein 'cleavage' mechanism indicates not a proteolytic reaction, but a novel translational effect: a putative ribosomal 'skip'. J. Gen. Virol. 82, 1013–1025.
Dunn, S.J., Cross, T.L., Greenberg, H.B., 1994. Comparison of the rotavirus non-structural protein NSP1 (NS53) from different species by sequence analysis and northern blot hybridization. Virology 203, 178–183.
Eiden, J.J., 1994. Expression and sequence analysis of gene 7 of the IDIR agent (group B rotavirus): similarity with NS53 of group A rotavirus. Virology 199, 212–218.
Estrozi, L.F., Settembre, E.C., Goret, G., McClain, B., Zhang, X., Chen, J.Z., Grigorieff, N., Harrison, S.C., 2013. Location of the dsRNA-dependent polymerase, VP1, in rotavirus particles. J. Mol. Biol. 425, 124–132.
Feng, N., Sen, A., Wolf, M., Vo, P., Hoshino, Y., Greenberg, H.B., 2011. Roles of VP4 and NSP1 in determining the distinctive replication capacities of simian rotavirus RRV and bovine rotavirus UK in the mouse biliary tract. J. Virol. 85, 2686–2694.
Feng, N., Yasukawa, L.L., Sen, A., Greenberg, H.B., 2013. Permissive replication of homologous murine rotavirus in the mouse intestine is primarily regulated by VP4 and NSP1. J. Virol. 87, 8307–8316.
Fink, K., Grandvaux, N., 2013. STAT2 and IRF9: beyond ISGF3. JAKSTAT 2, e27521.
Fukuhara, N., Nishikawa, K., Gorziglia, M., Kapikian, A.Z., 1989. Nucleotide sequence of gene segment 1 of a porcine rotavirus strain. Virology 173, 743–749.
Ghosh, S., Kobayashi, N., Nagashima, S., Chawla-Sarkar, M., Krishnan, T., Ganesh, B., Naik, T.N., 2010. Molecular characterization of the VP1, VP2, VP4, VP6, NSP1 and NSP2 genes of bovine group B rotaviruses: identification of a novel VP4 genotype. Arch. Virol. 155, 159–167.
Gilmore, B.L., Showalter, S.P., Dukes, M.J., Tanner, J.R., Demmert, A.C., McDonald, S.M., Kelly, D.F., 2013. Visualizing viral assemblies in a nanoscale biosphere. Lab Chip 13, 216–219.
Gold, M.G., Smith, F.D., Scott, J.D., Barford, D., 2008. AKAP18 contains a phosphoesterase domain that binds AMP. J. Mol. Biol. 375, 1329–1343.
Goubau, D., Deddouche, S., Reis e Sousa, C., 2013. Cytosolic sensing of viruses. Immunity 38, 855–869.
Graff, J.W., Ettayebi, K., Hardy, M.E., 2009. Rotavirus NSP1 inhibits NFkappaB activation by inducing proteasome-dependent degradation of beta-TrCP: a novel mechanism of IFN antagonism. PLoS Pathog. 5, e1000280.
Graff, J.W., Ewen, J., Ettayebi, K., Hardy, M.E., 2007. Zinc-binding domain of rotavirus NSP1 is required for proteasome-dependent degradation of IRF3 and autoregulatory NSP1 stability. J. Gen. Virol. 88, 613–620.
Graff, J.W., Mitzel, D.N., Weisend, C.M., Flenniken, M.L., Hardy, M.E., 2002. Interferon regulatory factor 3 is a cellular partner of rotavirus NSP1. J. Virol. 76, 9545–9550.
Gusho, E., Zhang, R., Jha, B.K., Thornbrough, J.M., Dong, B., Gaughan, C., Elliott, R., Weiss, S.R., Silverman, R.H., 2014. Murine AKAP7 has a 2′,5′-phosphodiesterase domain that can complement an inactive murine coronavirus ns2 gene. mBio 5, e01312–e01314.
Hayden, M.S., Ghosh, S., 2012. NF-kappaB, the first quarter-century: remarkable progress and outstanding questions. Genes Dev. 26, 203–234.
Hodel, A.E., Gershon, P.D., Shi, X., Quiocho, F.A., 1996. The 1.85A structure of vaccinia protein VP39: a bifunctional enzyme that participates in the modification of both mRNA ends. Cell 85, 247–256.
Holloway, G., Dang, V.T., Jans, D.A., Coulson, B.S., 2014. Rotavirus inhibits IFN-induced STAT nuclear translocation by a mechanism that acts after STAT binding to importin-alpha. J. Gen. Virol. 95, 1723–1733.
Holloway, G., Truong, T.T., Coulson, B.S., 2009. Rotavirus antagonizes cellular antiviral responses by inhibiting the nuclear accumulation of STAT1, STAT2, and NF-kappaB. J. Virol. 83, 4942–4951.
Hornung, V., Ellegast, J., Kim, S., Brzozka, K., Jung, A., Kato, H., Poeck, H., Akira, S., Conzelmann, K.K., Schlee, M., Endres, S., Hartmann, G., 2006. 5′-triphosphate RNA is the ligand for RIG-I. Science 314, 994–997.
Hoshino, Y., Saif, L.J., Kang, S.Y., Sereno, M.M., Chen, W.K., Kapikian, A.Z., 1995. Identification of group A rotavirus genes associated with virulence of a porcine rotavirus and host range restriction of a human rotavirus in the gnotobiotic piglet model. Virology 209, 274–280.
Hua, J., Chen, X., Patton, J.T., 1994. Deletion mapping of the rotavirus metalloprotein NS53 (NSP1): the conserved cysteine-rich region is essential for virus-specific RNA binding. J. Virol. 68, 3990–4000.
Hua, J., Mansell, E.A., Patton, J.T., 1993. Comparative analysis of the rotavirus NS53 gene: conservation of basic and cysteine-rich regions in the protein and possible stem-loop structures in the RNA. Virology 196, 372–378.
Hua, J., Patton, J.T., 1994. The carboxyl-half of the rotavirus nonstructural protein NS53 (NSP1) is not required for virus replication. Virology 198, 567–576.
Hundley, F., Biryahwaho, B., Gow, M., Desselberger, U., 1985. Genome rearrangements of bovine rotavirus after serial passage at high multiplicity of infection. Virology 143, 88–103.
Imai, M., Akatani, K., Ikegami, N., Furuichi, Y., 1983. Capped and conserved terminal structures in human rotavirus genome double-stranded RNA segments. J. Virol. 47, 125–136.
Ito, H., Sugiyama, M., Masubuchi, K., Mori, Y., Minamoto, N., 2001. Complete nucleotide sequence of a group A avian rotavirus genome and a comparison with its counterparts of mammalian rotaviruses. Virus Res. 75, 123–138.
Jiang, S., Ji, S., Tang, Q., Cui, X., Yang, H., Kan, B., Gao, S., 2008. Molecular characterization of a novel adult diarrhoea rotavirus strain J19 isolated in China and its significance for the evolution and origin of group B rotaviruses. J. Gen. Virol. 89, 2622–2629.
Kato, H., Takeuchi, O., Sato, S., Yoneyama, M., Yamamoto, M., Matsui, K., Uematsu, S., Jung, A., Kawai, T., Ishii, K.J., Yamaguchi, O., Otsu, K., Tsujimura, T., Koh, C.S., Reis e Sousa, C., Matsuura, Y., Fujita, T., Akira, S., 2006. Differential roles of MDA5 and RIG-I helicases in the recognition of RNA viruses. Nature 441, 101–105.
Kindler, E., Trojnar, E., Heckel, G., Otto, P.H., Johne, R., 2013. Analysis of rotavirus species diversity and evolution including the newly determined full-length genome sequences of rotavirus F and G. Infect. Genet. Evol. 14, 58–67.
Kobayashi, N., Naik, T.N., Kusuhara, Y., Krishnan, T., Sen, A., Bhattacharya, S.K., Taniguchi, K., Alam, M.M., Urasawa, T., Urasawa, S., 2001. Sequence analysis of genes encoding structural and nonstructural proteins of a human group B rotavirus detected in Calcutta, India. J. Med. Virol. 64, 583–588.
Kojima, K., Taniguchi, K., Kobayashi, N., 1996. Species-specific and interspecies relatedness of NSP1 sequences in human, porcine, bovine, feline, and equine rotavirus strains. Arch. Virol. 141, 1–12.
Langland, J.O., Pettiford, S., Jiang, B., Jacobs, B.L., 1994. Products of the porcine group C rotavirus NSP3 gene bind specifically to double-stranded RNA and inhibit activation of the interferon-induced protein kinase PKR. J. Virol. 68, 3821–3829.
Liu, M., Mattion, N.M., Estes, M.K., 1992. Rotavirus VP3 expressed in insect cells possesses guanylyltransferase activity. Virology 188, 77–84.
Lu, X., McDonald, S.M., Tortorici, M.A., Tao, Y.J., Vasquez-Del Carpio, R., Nibert, M.L., Patton, J.T., Harrison, S.C., 2008. Mechanism for coordinated RNA packaging and genome replication by rotavirus polymerase VP1. Structure 16, 1678–1688.
Matthijnssens, J., Otto, P.H., Ciarlet, M., Desselberger, U., Van Ranst, M., Johne, R., 2012. VP6-sequence-based cutoff values as a criterion for rotavirus species demarcation. Arch. Virol. 157, 1177–1182.
Mazumder, R., Iyer, L.M., Vasudevan, S., Aravind, L., 2002. Detection of novel members, structure-function analysis and evolutionary classification of the 2H phosphoesterase superfamily. Nucleic Acids Res. 30, 5229–5243.
McClain, B., Settembre, E., Temple, B.R., Bellamy, A.R., Harrison, S.C., 2010. X-ray crystal structure of the rotavirus inner capsid particle at 3.8A resolution. J. Mol. Biol. 397, 587–599.
Mitchell, D.B., Both, G.W., 1990. Conservation of a potential metal binding motif despite extensive sequence diversity in the rotavirus nonstructural protein NS53. Virology 174, 618–621.
Nandi, S., Chanda, S., Bagchi, P., Nayak, M.K., Bhowmick, R., Chawla-Sarkar, M., 2014. MAVS protein is attenuated by rotavirus nonstructural protein 1. PLoS One 9, e92126.
Ogden, K.M., Snyder, M.J., Dennis, A.F., Patton, J.T., 2014. Predicted structure and domain organization of rotavirus capping enzyme and innate immune antagonist VP3. J. Virol. 88, 9072–9085.

Patton, J.T., Chen, D., 1999. RNA-binding and capping activities of proteins in rotavirus open cores. J. Virol. 73, 1382–1391.
Patton, J.T., Silvestri, L.S., Tortorici, M.A., Vasquez-Del Carpio, R., Taraporewala, Z.F., 2006. Rotavirus genome replication and morphogenesis: role of the viroplasm. Curr. Top. Microbiol. Immunol. 309, 169–187.
Patton, J.T., Taraporewala, Z., Chen, D., Chizhikov, V., Jones, M., Elhelu, A., Collins, M., Kearney, K., Wagner, M., Hoshino, Y., Gouvea, V., 2001. Effect of intragenic rearrangement and changes in the 3′ consensus sequence on NSP1 expression and rotavirus replication. J. Virol. 75, 2076–2086.
Phan, T.G., Vo, N.P., Boros, A., Pankovics, P., Reuter, G., Li, O.T., Wang, C., Deng, X., Poon, L.L., Delwart, E., 2013. The viruses of wild pigeon droppings. PLoS One 8, e72787.
Pichlmair, A., Schulz, O., Tan, C.P., Naslund, T.I., Liljestrom, P., Weber, F., Reis e Sousa, C., 2006. RIG-I-mediated antiviral responses to single-stranded RNA bearing 5′-phosphates. Science 314, 997–1001.
Pizarro, J.L., Sandino, A.M., Pizarro, J.M., Fernandez, J., Spencer, E., 1991. Characterization of rotavirus guanylyltransferase activity associated with polypeptide VP3. J. Gen. Virol. 72, 325–332.
Prasad, B.V., Rothnagel, R., Zeng, C.Q., Jakana, J., Lawton, J.A., Chiu, W., Estes, M.K., 1996. Visualization of ordered genomic RNA and localization of transcriptional complexes in rotavirus. Nature 382, 471–473.
Qin, B.Y., Liu, C., Lam, S.S., Srinath, H., Delston, R., Correia, J.J., Derynck, R., Lin, K., 2003. Crystal structure of IRF-3 reveals mechanism of autoinhibition and virus-induced phosphoactivation. Nat. Struct. Biol. 10, 913–921.
Qin, L., Ren, L., Zhou, Z., Lei, X., Chen, L., Xue, Q., Liu, X., Wang, J., Hung, T., 2011. Rotavirus nonstructural protein 1 antagonizes innate immune response by interacting with retinoic acid inducible gene I. Virol J. 8, 526.
Reikine, S., Nguyen, J.B., Modis, Y., 2014. Pattern recognition and signaling mechanisms of RIG-I and MDA5. Front. Immunol. 5, 342.
Rivas, C., Aaronson, S.A., Munoz-Fontela, C., 2010. Dual Role of p53 in innate antiviral immunity. Viruses 2, 298–313.
Savitsky, D., Tamura, T., Yanai, H., Taniguchi, T., 2010. Regulation of immunity and oncogenesis by the IRF transcription factor family. Cancer Immunol. Immunother. 59, 489–510.
Sen, A., Feng, N., Ettayebi, K., Hardy, M.E., Greenberg, H.B., 2009. IRF3 inhibition by rotavirus NSP1 is host cell and virus strain dependent but independent of NSP1 proteasomal degradation. J. Virol. 83, 10322–10335.
Sen, A., Pruijssers, A.J., Dermody, T.S., Garcia-Sastre, A., Greenberg, H.B., 2011. The early interferon response to rotavirus is regulated by PKR and depends on MAVS/IPS-1, RIG-I, MDA-5, and IRF3. J. Virol. 85, 3717–3732.
Shen, S., McKee, T.A., Wang, Z.D., Desselberger, U., Liu, D.X., 1999. Sequence analysis and in vitro expression of genes 6 and 11 of an ovine group B rotavirus isolate, KB63: evidence for a non-defective, C-terminally truncated NSP1 and a phosphorylated NSP5. J. Gen. Virol. 80, 2077–2085.
Silverman, R.H., 2007. Viral encounters with 2′,5′-oligoadenylate synthetase and RNase L during the interferon antiviral response. J. Virol. 81, 12720–12729.
Silverman, R.H., Weiss, S.R., 2014. Viral phosphodiesterases that antagonize double-stranded RNA signaling to RNase L by degrading 2-5A. J. Interferon Cytokine Res. 34, 455–463.
Soma, J., Tsunemitsu, H., Miyamoto, T., Suzuki, G., Sasaki, T., Suzuki, T., 2013. Whole-genome analysis of two bovine rotavirus C strains: Shintoku and Toyama. J. Gen. Virol. 94, 128–135.
Spencer, E., Garcia, B.I., 1984. Effect of S-adenosylmethionine on human rotavirus RNA synthesis. J. Virol. 52, 188–197.
Subodh, S., Bhan, M.K., Ray, P., 2006. Genetic characterization of VP3 gene of group A rotaviruses. Virus Genes 33, 143–145.
Sutton, G., Grimes, J.M., Stuart, D.I., Roy, P., 2007. Bluetongue virus VP4 is an RNA-capping assembly line. Nat. Struct. Mol. Biol. 14, 449–451.
Takagi, T., Moore, C.R., Diehn, F., Buratowski, S., 1997. An RNA 5′-triphosphatase related to the protein tyrosine phosphatases. Cell 89, 867–873.
Takeuchi, O., Akira, S., 2010. Pattern recognition receptors and inflammation. Cell 140, 805–820.
Taniguchi, K., Kojima, K., Urasawa, S., 1996. Nondefective rotavirus mutants with an NSP1 gene which has a deletion of 500 nucleotides, including a cysteine-rich zinc finger motif-encoding region (nucleotides 156 to 248), or which has a nonsense codon at nucleotides 153–155. J. Virol. 70, 4125–4130.
Tate, J.E., Burton, A.H., Boschi-Pinto, C., Steele, A.D., Duque, J., Parashar, U.D., WHO-coordinated Global Rotavirus Surveillance Network, 2012. 2008 estimate of worldwide rotavirus-associated mortality in children younger than 5 years before the introduction of universal rotavirus vaccination programmes: a systematic review and meta-analysis. Lancet Infect. Dis. 12, 136–141.
Taylor, K.E., Mossman, K.L., 2013. Recent advances in understanding viral evasion of type I interferon. Immunology 138, 190–197.
Tian, Y., Tarlow, O., Ballard, A., Desselberger, U., McCrae, M.A., 1993. Genomic concatemerization/deletion in rotaviruses: a new mechanism for generating rapid genetic change of potential epidemiological importance. J. Virol. 67, 6625–6632.
Trask, S.D., McDonald, S.M., Patton, J.T., 2012. Structural insights into the coupling of virion assembly and rotavirus replication. Nat. Rev. Microbiol. 10, 165–177.
Trojnar, E., Otto, P., Johne, R., 2009. The first complete genome sequence of a chicken group A rotavirus indicates independent evolution of mammalian and avian strains. Virology 386, 325–333.
Trojnar, E., Otto, P., Roth, B., Reetz, J., Johne, R., 2010. The genome segments of a group D rotavirus possess group A-like conserved termini but encode group-specific proteins. J. Virol. 84, 10254–10265.
Uzri, D., Greenberg, H.B., 2013. Characterization of rotavirus RNAs that activate innate immune signaling through the RIG-I-like receptors. PLoS One 8, e69825.
Wang, W., Donnelly, B., Bondoc, A., Mohanty, S.K., McNeal, M., Ward, R., Sestak, K., Zheng, S., Tiao, G., 2011. The rhesus rotavirus gene encoding VP4 is a major determinant in the pathogenesis of biliary atresia in newborn mice. J. Virol. 85, 9069–9077.
Xie, P., 2013. TRAF molecules in cell signaling and in human diseases. J. Mol. Signal. 8, 7.
Yang, H., Makeyev, E.V., Kang, Z., Ji, S., Bamford, D.H., van Dijk, A.A., 2004. Cloning and sequence analysis of dsRNA segments 5, 6 and 7 of a novel non-group A, B, C adult rotavirus that caused an outbreak of gastroenteritis in China. Virus Res. 106, 15–26.
Yu, J., Wjasow, C., Backer, J.M., 1998. Regulation of the p85/p110alpha phosphatidylinositol 3′-kinase. Distinct roles for the n-terminal and c-terminal SH2 domains. J. Biol. Chem. 273, 30199–30203.
Zeng, C.Q., Estes, M.K., Charpilienne, A., Cohen, J., 1998. The N terminus of rotavirus VP2 is necessary for encapsidation of VP1 and VP3. J. Virol. 72, 201–208.
Zhang, R., Jha, B.K., Ogden, K.M., Dong, B., Zhao, L., Elliott, R., Patton, J.T., Silverman, R.H., Weiss, S.R., 2013. Homologous 2′,5′-phosphodiesterases from disparate RNA viruses antagonize antiviral innate immunity. Proc. Natl. Acad. Sci. USA 110, 13114–13119.
Zhao, L., Jha, B.K., Wu, A., Elliott, R., Ziebuhr, J., Gorbalenya, A.E., Silverman, R.H., Weiss, S.R., 2012. Antagonism of the interferon-induced OAS-RNase L pathway by murine coronavirus ns2 protein is required for virus replication and liver pathology. Cell Host Microbe 11, 607–616.